

Sky Dancer: A Complex Fluid-Structure Interaction

Anne Cros, Jesse Alexander Rodríguez Romero
and Fernando Castillo Flores

Abstract Sky dancers are long vertical flexible tubes which fluctuate above an air blower. These systems involve fluid-structure interactions that can give rise to complex dynamics. Air flow which passes through the tube deforms the tube wall which in turn modifies the flow hydrodynamical properties, and so on. We present in this article an experiment which models a sky dancer. The blown air speed can be varied and tubes of low rigidity and of different dimensions are used. The critical values of the flow velocity for which each tube begins “dancing” are measured. Comparisons with previous theoretical studies conducted for much more rigid tubes (Païdoussis, *J Sound Vib* 33:267–294, 1970) allow us to show that for tubes of low rigidity, the mechanism of destabilization is different.

1 Introduction

One of the first studies about the instability of pipes conducting flows was published by Ashley and Haviland (1950) in an attempt to explain vibrations which appear in pipelines. For half a century, studies about this kind of system have become more and more numerous (Païdoussis 1998). Indeed, many practical applications can be modeled by this kind of system as, for example, pipelines or heat transfer systems used in aircraft engines and nuclear reactors. Other typical examples can be found in biomechanics as blood flows in veins or air flow in pulmonary alveolus. This kind of instability can also be observed in everyday life

A. Cros (✉) · J. A. R. Romero · F. C. Flores
Departamento de Física, Universidad de Guadalajara, Av. Revolución
1500 Col., Olímpica, 44430 Guadalajara, Jalisco, México
e-mail: anne@astro.iam.udg.mx

when we water the garden and let the pipe loose: if the flow is sufficient, the garden-hose will fluctuate, making snake-like undulations.

The sky dancers are another example of such an instability. Sky dancers are long flexible tubes, made with ripstop fabrics, which fluctuate in streets as advertising. They “dance” above an air blower to advertise a product.

Previous works about slender structures and axial flow interaction are extensively reviewed by Paidoussis (1998). We present here theoretical and experimental results related to the present work.

1.1 Theoretical Studies

Let consider a tube with mass per unit length m_t (kg/m) and flexural rigidity EI (N.m²), where E is the Young’s modulus of the material and I the second moment of inertia of the tube section. This pipe conducts a fluid and the mass of fluid contained per unit length of pipe is noted m_f . This fluid flows with velocity v in the pipe. Now let us call $w(x, t)$ the transversal displacement of the pipe from its vertical position, where x is the longitudinal coordinate (vertical ascending in the present study) and t is the time. If gravity, dissipation and pressurization effects are neglected and if air velocity v is considered as being constant, the governing equation for the pipe motion writes:

$$EI \frac{\partial^4 w}{\partial x^4} + m_f v^2 \frac{\partial^2 w}{\partial x^2} + 2m_f v \frac{\partial^2 w}{\partial x \partial t} + (m_f + m_t) \frac{\partial^2 w}{\partial t^2} = 0 \quad (1)$$

The first term corresponds to internal forces in the tube generated by the pipe flexural rigidity. These forces tend to make the tube return to its straight vertical position. The second term corresponds to the centrifugal force. Indeed $\partial^2 w / \partial X^2 \sim 1/R$, where R is the local curvature radius. This force is the same as the reaction generated by the flow on a curved rigid surface. It is directed towards the tube convex curvature and is destabilizing. The third term corresponds to the Coriolis force. Indeed $\partial w / \partial X \sim \theta$, where θ is the tube angle with respect to vertical, so that $\partial^2 w / \partial X \partial t \sim \Omega$, where $\Omega = \partial \theta / \partial t$ is the angular velocity of a tube element. The Coriolis force is always opposing the tube movement. The last term represents the inertial forces of the system pipe and fluid.

Theoretical studies (Gregory and Paidoussis 1966a; Paidoussis 1966, 1969; Paidoussis and Issid 1974) show that in case of cantilevers, the system is governed by three nondimensional parameters, the nondimensional velocity

$$u = \left(\frac{m_f}{EI} \right)^{1/2} L v \quad (2)$$

the gravity parameter

$$\gamma = \frac{(m_f + m_t)L^3}{EI}g \quad (3)$$

and the mass ratio

$$\beta = \frac{m_f}{m_f + m_t} \quad (4)$$

Païdoussis (1970) takes the convention $\gamma > 0$ when the tube hangs and $\gamma < 0$ when the tube stands up. In this theoretical work, Païdoussis finds that for $0 < |\gamma| < 7.83$, the tube is stable for low values of flow velocities v and unstable above a threshold which depends upon β and γ . Nevertheless if the tube length is such that $7.83 < |\gamma| < 55.9$, the tube falls down because of its own weight for low velocity values. If velocity is increased the tube stands up for short enough tubes, then it fluctuates at higher velocities. For the longest tubes, the rising-up regime never happens and the air flow makes the tube fluctuate when the velocity is large enough.

The thresholds between the different regimes depend upon β and γ . The threshold u_{cf} for “fluttering” region is higher if β is greater. That is to say that it is more difficult to destabilize a slighter tube. Moreover, the stability curves delimiting the fluctuating region from the other ones are such that u_{cf} is a decreasing function of $|\gamma|$: a long tube is easier to destabilize than a short one.

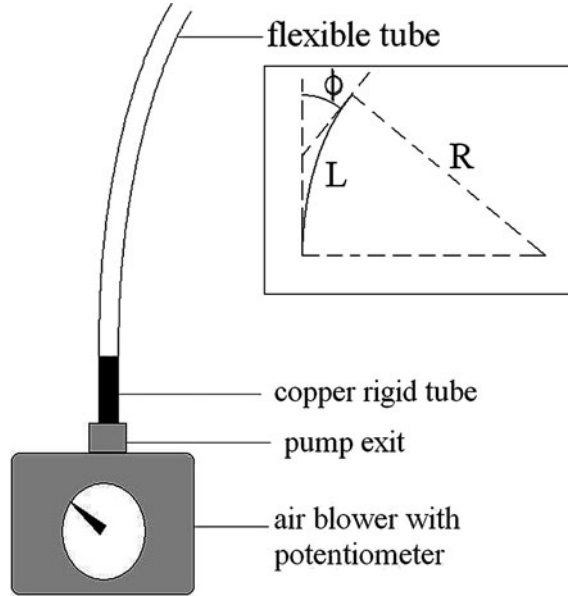
1.2 Experimental Works

Experiments were conducted by Païdoussis (1963) and Gregory and Païdoussis (1966b) with horizontal pipes. Those authors used rubber and metal pipes, conveying air or water. Pipes of internal diameter from 1 to 13 mm and of thickness extending from 0.8 to about 3 mm were used. The pipe length was varied from 20 to 76 cm. We will see that our tubes have roughly the same lengths but have a greater diameter, a thinner wall, and a very low rigidity (very low Young modulus).

Those authors reported, particularly in the case of rubber pipes, hysteresis behavior: the pipe persisted oscillating below the threshold value when flow intensity was decreased. This suggests that the Hopf bifurcation is subcritical (Païdoussis 1998, p. 134).

We can also mention the experimental works with hanging pipes of Greenwald and Dugundji (1967) or Doaré and de Langre (2002). Nevertheless, results of the present study can only be compared to those of Païdoussis (1970) since this last study includes experiments with hanging and standing pipes. Only this last configuration is similar to the case investigated in this paper.

Fig. 1 Experimental system: the air blower is connected to 110 V, and a potentiometer permits variation of the air velocity. Copper cylinders of different diameters can be connected to the pump exit and the flexible tubes are made to adapt the copper tubes. The insert shows tube length L , deviation angle ϕ and curvature radius R



2 Experimental Device

The set-up used in the present experiments is schematically shown in Fig. 1. It consists in a centrifugal air blower coupled to a potentiometer to allow the variation of the pump power and thus of the air flow velocity. This velocity can be varied from 0 to 40 m/s if no charge is connected at the pump. The blower exit diameter is 4 cm and various copper connections are used to adjust to flexible tubes of different diameters. Tubes of diameters $d = 4.0, 2.9, 2.2$ and 1.5 cm have been used, their length L was varied from 0.35 to 1.0 m.

Flexible tubes are made with a plastic membrane. The measured characteristics for this material were a thickness e of 0.1 mm, a surface density ρ_s of 0.083 kg/m² and a Young modulus E of 4.5 MPa. The tubes were made sealing the plastic membrane with heat, so that membrane was superimposed along the tube over less than 1 mm. In comparison to the sticking technique described in Castillo Flores and Cros (2009), the heat-sealing technique presently used allows to avoid a rigid band formation along the tube and the formation of a slight curvature effect. We found in our experiments that tubes as long as 1 m and as slim as 1.5 cm diameter could stand up with an adequate air speed. This shows that the tubes we made were straight enough.

The experimental procedure was the following. A flexible tube was connected to the pump exit, then the flow velocity was quasi-statically increased from 0.

The tube was first observed to be stable (did not fall down because of its own weight). Then at a critical value of the flow velocity, the tube began oscillating. At this value, we introduce in the free end of the flexible tube two thin pipes, each one connected to a manometer, in order to measure the dynamical pressure p_d and the static pressure p . The critical velocity v could then be estimated from these measurements by means of the following relation:

$$v = \sqrt{\frac{2(p_d - p)}{\rho}} \quad (5)$$

where ρ is the air density.

3 Results

3.1 Observations

For each tube length and each critical air velocity value, at the threshold of the instability, we record the transient dynamics with a video camera. So we visualize how the tube evolves from a raised, immobile state, to the instant when the tube falls down and “breaks”. Figure 2 illustrates the tube transient dynamics.

Figure 2 shows the tube position only for the last oscillation cycle. We counted for this video four cycles before the first picture of Fig. 2. The tube begins oscillating with very small amplitude which increases with time. For the last oscillation cycle, amplitude is so great that the tube breaks (that is, a singularity appears along the tube), as shown in the tenth and last pictures.

This transient dynamics was not observed by Castillo Flores and Cros (2009). In this previous study, we saw that the tube collapsed locally at its basis (that is, where it is fixed to the pump exit) and that the constriction point climbed upwards to the free extreme of the tube. It is suspected that this difference is due to the tube manufacture previously used. This later resulted in a slight curvature defect that has been strongly reduced with the manufacture process described above (see Sect. 2).

So we observe that in the transient dynamics, the tube is destabilized in the same way as the tubes with higher rigidity: it fluctuates with a certain periodicity and with a continuous spatial shape, until it breaks. From these observations, we can deduce that the instability which appears in our slim flexible tubes is of the same nature as that described by previous studies (Païdoussis 1970). Nevertheless, the threshold values do not agree with this theory, as it is shown in the next section.

3.2 Thresholds

Experiments have been performed with four different diameters $d = 1.5, 2.2, 2.9$ and 4.0 cm. Nevertheless we have not been able to observe any instability for the

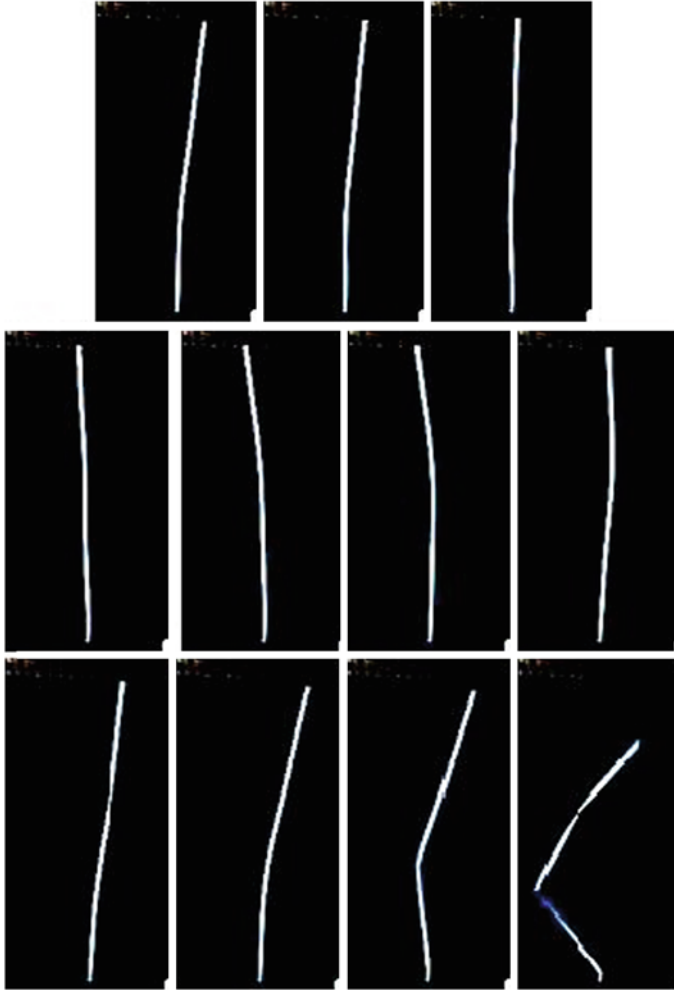


Fig. 2 Tube transient dynamics just at the threshold, before it breaks (*final picture*). Those pictures are extracted from a video corresponding to a 1 m-long, 1.5 cm-diameter tube. There is a lapse of 230 ms between each picture

tubes of diameter $d = 4.0$ cm because of the air speed values that can be reached by our air blower.

Figure 3 shows the thresholds v_c measured in our system for tubes of different diameters and lengths. Firstly, we observe that tubes of greater diameter are more stable than slim tubes. For example, for tubes of length $L = 0.95$ m, the critical velocity is $v_c = 32.8$ m/s for a diameter $d = 2.9$ cm, whereas it is of 27.7 m/s for $d = 2.2$ cm and of 20.9 m/s for $d = 1.5$ cm. This result is in agreement with Païdoussis's observations (see Sect. 1.1). Indeed as diameter d is increased,

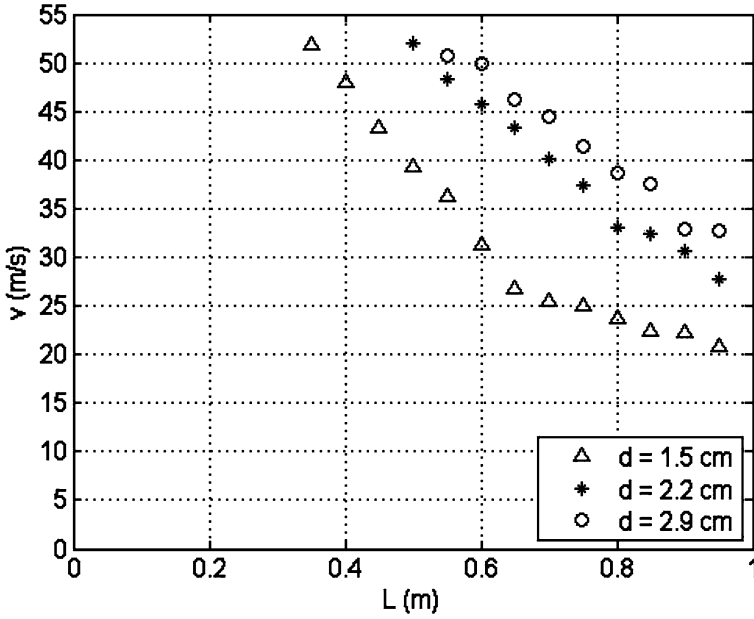


Fig. 3 Threshold values for tubes with different diameters: (Δ) 1.5 cm, ($*$) 2.2 cm, (\circ) 2.9 cm. *x-axis*: tube length L (m), *y-axis*: air velocity v_c (m/s) at instability threshold

parameter β (Eq. 4) increases, as seen in Table 1, and the instability threshold is greater.

Moreover, Fig. 3 shows that shorter tubes are more stable since they need higher air speeds to be destabilized. It should be pointed out that our air blower did not allow to reach threshold values for tubes shorter than 0.35 m. These observations are also in agreement with Païdoussis's results.

4 Analysis

In this section, a scaling analysis is conducted in order to emphasize the predominant stabilizing and destabilizing effects involved in the observed instability.

As described in the introduction (Sect. 1.1), destabilization is caused by centrifugal effects. Let us imagine a curved rigid tube conveying air flow. If air flow is deviated by an angle ϕ as shown in Fig. 1, momentum conservation leads to a horizontal force F which acts on the tube and is given by:

$$F = A\rho v^2 \sin \phi \quad (6)$$

where A is the tube cross-section and ρ the fluid density. This force component always acts in the convex direction: for example in Fig. 1, F is leftwards directed.

Table 1 Flexural rigidity values EI for the three different diameters and values for β (Eq. 4)

d (cm)	1.5	2.2	2.9
EI (10^{-4} Nm ²)	6	21	42
β	0.052	0.076	0.095

On the other hand tube stiffness makes the tube return to its straight position. Internal moment M generated by a radius R -curved tube can be written as:

$$M = \frac{EI}{R} \quad (7)$$

where EI is the tube flexural rigidity. For small Φ angles, that is to say large R curvature radius, we can show geometrically that:

$$\frac{1}{R} = \frac{\phi}{L} \quad (8)$$

Therefore, a characteristic force F_{EI} for flexural rigidity is given by:

$$F_{EI} = \frac{EI\phi}{L^2} \quad (9)$$

Finally the ratio Q between the destabilizing force (Eq. 6) and the stabilizing force (Eq. 9) for small tube deviations can be written as:

$$Q = \frac{A\rho v^2 L^2}{EI} \quad (10)$$

Remembering that $m_f = \rho A$, this ratio appears to be the squared value of the nondimensional velocity u defined in Eq. 2.

The nondimensional critical values of the flow velocity are plotted in Fig. 4 as function of the nondimensional parameter γ introduced by Païdoussis (1998).

For these results, the flexural rigidity EI was determined with the measured value of the Young modulus $E = 4.5$ MPa and with the following formula for the second moment of inertia

$$I = \frac{\pi}{4}(r^4 - (r - e)^4) \quad (11)$$

where r is the tube radius and e the membrane thickness. Table 1 shows the corresponding values for EI and β for the three different diameters.

We can see in Fig. 4 that the points for $d = 2.2$ and 2.9 cm collapse on a single curve. The values for $d = 1.5$ cm are close to but smaller than both the other series. Nevertheless it is not expected theoretically that the three point series strictly superimpose since they correspond to different β values. It is expected that series relatively close together have similar β values, and this is observed experimentally.

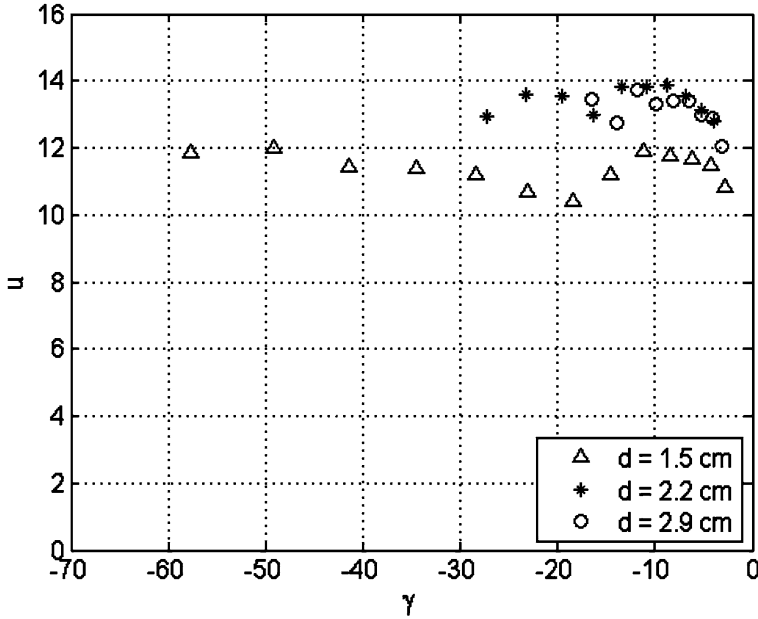


Fig. 4 Nondimensional critical flow velocities u as function of the nondimensional parameter γ for different tubes

Even so, the results found by Païdoussis (1970) are different. For our β experimental values shown in Table 1, theoretical nondimensional thresholds u vary between 0 and 4 and increase as $|\gamma|$ decreases. We can see that the thresholds in our case are three times higher than the predicted values. Moreover u is roughly constant in our experiment. We do not know yet how to explain these discrepancies.

5 Conclusion and Perspectives

In this work, we have experimentally measured the instability thresholds for a reduced “sky dancer” model. The measurements have been performed for various tube lengths and three different diameters. We have plotted the nondimensional critical velocities as function of the nondimensional parameter γ introduced by Païdoussis (1970) in a study concerning more rigid tubes. This allowed to show that the results strongly differ when much less rigid tubes are considered.

In order to characterize the instability mechanism which makes the tube “break”, we should in future take into account the following considerations:

1. We will measure thresholds with a more precise apparatus like a hot-wire anemometer. This will reduce the uncertainty on measured thresholds.

2. We also want to measure pressure values on the tube base at the instability thresholds. This experimental system appears cheap and simple at first sight, but it is also more complex because both pressure and air speed vary simultaneously.
3. On the other hand we want to determine the flexural rigidity EI in a completely experimental way. A method is given by Païdoussis (1998). Indeed the slight overlapped membrane region along the tube may make EI values higher than the calculated ones in Table 1. This could change values on the x -axis.
4. We will also perform new experiments with another membrane to check the influence of Young modulus.
5. Another parameter we could compare with Païdoussis' theoretical work is oscillation frequency in the transient regime. This could help us to explain discrepancies and similarities between our experiment and the previous studies.
6. Finally we should also characterize the thresholds which delimit other two regimes: when the tube falls down because of its own weight (large tubes, small air speed values) and when the tube stands up. In the present study we were only interested in the thresholds delimiting the raised-tube regime from the "instability" regime, where the flow makes the tube "dance".

References

- Ashley H, Haviland G (1950) Bending vibrations of a pipe line containing flowing fluid. *J Appl Mech* 17:229–232
- Castillo Flores F, Cros A (2009) Transition to chaos of a vertical collapsible tube conveying air flow. *J Phys Conf Ser* 166:012017
- Doaré O, de Langre E (2002) The flow-induced instability of long hanging pipes. *Eur J Mech A Solids* 21:857–867
- Greenwald AS, Dugundji J (1967) Static and dynamic instabilities of a propellant line. MIT Aeroelastic and Structures Research Lab, AFOSR Sci Report: AFOSR 67-1395
- Gregory RW, Païdoussis MP (1966a) Unstable oscillation of tubular cantilevers conveying fluid. I. Theory. *Proc R Soc (London) A* 293:512–527
- Gregory RW, Païdoussis MP (1966b) Unstable oscillation of tubular cantilevers conveying fluid. II. Experiments. *Proc R Soc (London) A* 293:528–542
- Païdoussis MP (1963) Oscillations of liquid-filled flexible tubes. Ph. D. Thesis, University of Cambridge
- Païdoussis MP (1966) Dynamics of flexible slender cylinders in axial flow. Part 1: theory. *J Fluid Mech* 26:717–736
- Païdoussis MP (1969) Dynamics of vertical tubular cantilevers conveying fluid. Mechanical engineering research laboratories report MERL, Department of Mechanical Engineering, McGill University, Montreal, Québec, Canada, pp 69–73
- Païdoussis MP (1970) Dynamics of tubular cantilevers conveying fluid. *Int J Mech Eng Sci* 12:85–103
- Païdoussis MP, Issid NT (1974) Dynamic stability of pipes conveying fluid. *J Sound Vib* 33:267–294
- Païdoussis MP (1998) Fluid-Structure interactions. Slender structures and axial flow, vol 1. Academic Press, London

Experimental and Theoretical Advances in Fluid
Dynamics

Klapp, J.; Cros, A.; Velasco Fuentes, O.; Stern, C.;
Rodriguez Meza, M.A. (Eds.)

2012, XXII, 518 p., Hardcover

ISBN: 978-3-642-17957-0